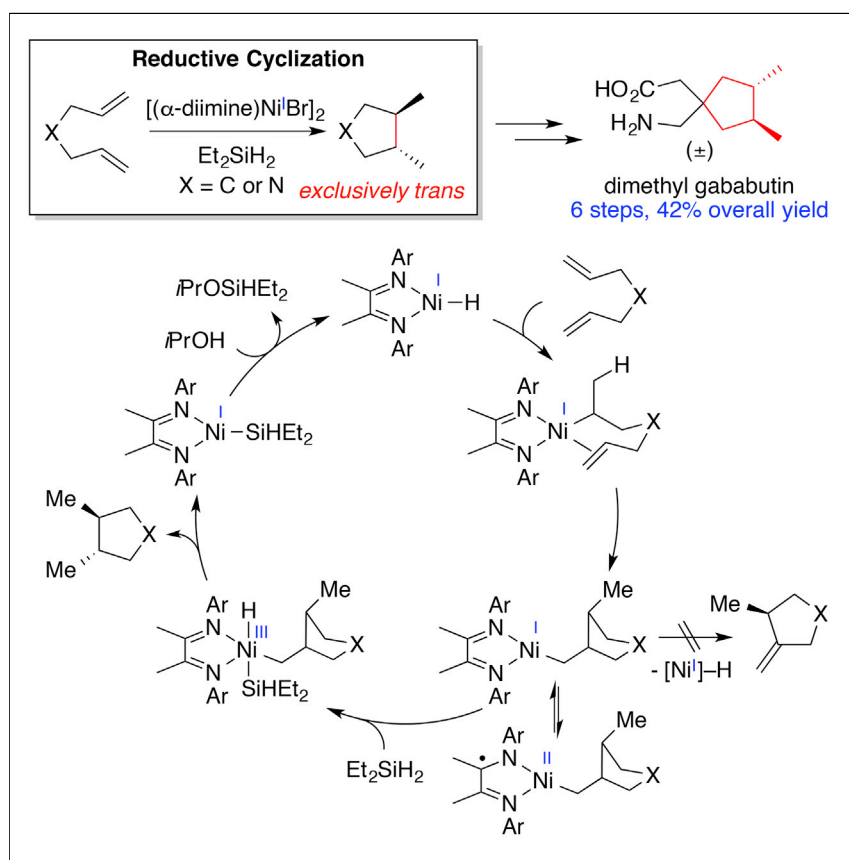


## Article

# Ni(I)-Catalyzed Reductive Cyclization of 1,6-Dienes: Mechanism-Controlled *trans* Selectivity



Yulong Kuang, David Anthony,  
Joseph Katigbak, Flaminia  
Marrucci, Sunita Humagain,  
Tianning Diao

diao@nyu.edu

## HIGHLIGHTS

Reductive coupling of dienes gives a *trans* diastereoselectivity

An efficient synthesis of a gababutin derivative for treating neuropathic pain

A classic organometallic mechanism is mediated by Ni(I) and Ni(III) intermediates

The mechanistic basis for the chemoselectivity and diastereoselectivity

Diao and coworkers have developed a reductive coupling reaction to convert 1,6-dienes into cyclic molecules with *trans*-vicinal disubstituents. This method is readily applicable to the syntheses of biologically active molecules with high efficiency. Mechanistic studies revealed that the reaction proceeds via a classic, two-electron transfer mechanism mediated by paramagnetic Ni(I) and Ni(III) intermediates. The identification of the well-defined Ni(I) catalyst and elucidation of the mechanism will facilitate future development of Ni-catalyzed cross-coupling reactions.



## Article

# Ni(I)-Catalyzed Reductive Cyclization of 1,6-Dienes: Mechanism-Controlled *trans* Selectivity

Yulong Kuang,<sup>1</sup> David Anthony,<sup>1</sup> Joseph Katigbak,<sup>1</sup> Flaminia Marrucci,<sup>1</sup> Sunita Humagain,<sup>2</sup> and Tianning Diao<sup>1,3,\*</sup>

## SUMMARY

A Ni-catalyzed reductive cyclization of 1,6-dienes affords 3,4-disubstituted cyclopentane and pyrrolidine derivatives with high *trans* diastereoselectivity. This cyclization reaction enables the efficient synthesis of *trans*-3,4-dimethyl gababutin, a pharmaceutical lead for treating neuropathic pain, and *trans*-3,4-dimethylpyrrolidine, a precursor to drug candidates and pesticides. The *trans* selectivity distinguishes this reaction from relevant precedents that proceed via hydrogen-atom transfer and lead to *cis* products. Mechanistic investigation, including kinetic, spectroscopic, and radical clock studies, attributes the *trans* diastereoselectivity to a classic, organometallic catalytic cycle mediated by Ni(I) and Ni(III) intermediates. The electron-rich Ni(I) intermediate, stabilized by a redox-active  $\alpha$ -diimine ligand, is responsible for the chemoselectivity toward reductive cyclization as opposed to the redox-neutral cycloisomerization observed with previous Ni(II) catalysts.

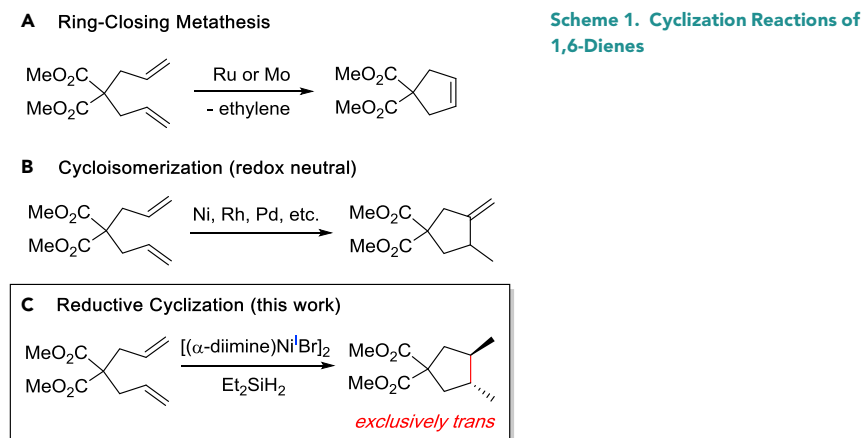
## INTRODUCTION

Contemporary nickel-catalyzed cross-coupling reactions have found widespread applications in organic synthesis.<sup>1,2</sup> The mechanisms of these reactions frequently invoke single-electron transfer steps and Ni(I) and Ni(III) intermediates.<sup>3,4</sup> In contrast to radical pathways, the mechanism for Ni(0)-catalyzed reductive coupling of unsaturated molecules, developed by Montgomery and colleagues,<sup>5</sup> proceeds through classic oxidative cycloaddition of Ni(0) to form Ni(II) metallocycles. Although these reactions provide an appealing way to functionalize alkynes, similar reactivity has not been observed with unactivated alkenes. Here, we report a reductive cyclization of dienes that proceeds via a mechanism distinct from those of previous reports. A well-defined Ni(I) intermediate mediates two-electron transfer pathways via a Ni(I)-Ni(III) catalytic cycle, without single-electron transfers and organic radical intermediates.

Alkenes are versatile functional groups in organic synthesis. Catalytic functionalization of alkenes represents one of the most powerful synthetic strategies in contemporary pharmaceutical synthesis. Cyclization reactions of olefins can rapidly construct cyclic molecules and have been practiced extensively. Among a variety of approaches, ring-closing metathesis is the most widespread, giving rise to unsaturated ring systems (Scheme 1A).<sup>6,7</sup> In addition, [2 + 2] cycloaddition and ene reactions provide access to a variety of cycles.<sup>8,9</sup> A number of catalytic conditions have been developed to carry out the cycloisomerization of dienes to form exo-methylene-cyclopentanes (Scheme 1B).<sup>10,11</sup> In particular, Widenhoefer and DeCarli<sup>12</sup> and

## The Bigger Picture

Modern pharmaceutical and chemical synthesis calls for new catalytic methods of accessing intricate molecules with high efficiency. Ni-catalyzed cross-coupling reactions have emerged as an appealing method for the construction of C–C bonds. The complex mechanisms of these reactions often involve single-electron transfer and radical intermediates. Here, we used a well-defined Ni(I) complex to catalyze a *trans*-selective reductive coupling of dienes, which led to the efficient synthesis of biologically active molecules. The reaction proceeds via a classic, two-electron transfer pathway mediated by paramagnetic Ni(I) and Ni(III) intermediates. This mechanism distinguishes this work from previous reactions and accounts for the observed *trans* diastereoselectivity and the chemoselectivity for reductive coupling. The characterization of this mechanism and the introduction of the Ni(I) catalyst precursor are anticipated to inspire catalyst design in the field of Ni catalysis.



Perch et al.<sup>13</sup> used Pd(II) catalysts to perform cyclization of dienes, followed by a tandem coupling with silanes to afford *cis*-disubstituted silylated products. A recent report by Crossley et al.<sup>14</sup> shows that Co catalyzes cycloisomerization via hydrogen atom transfer (HAT) to afford *cis*-3,4-disubstituted cyclopentanes. Reductive coupling of unactivated alkenes can install two adjacent stereocenters at once, but such reactivity has been historically challenging (Scheme 1C).<sup>15–17</sup>

*trans*-3,4-Disubstituted cyclopentane<sup>18</sup> and pyrrolidine motifs are commonplace in natural products and pharmaceutical leads.<sup>19,20</sup> Synthesis of *trans*-3,4-disubstituted five-membered rings, however, often requires multiple steps<sup>21,22</sup> or stoichiometric metal reagents.<sup>23</sup> Using the Ni(I)/Ni(III)-mediated two-electron mechanism, we developed a reductive cyclization of 1,6-dienes, which provides *trans*-3,4-disubstituted cyclopentane and pyrrolidine derivatives (Scheme 1C). The *trans* diastereoselectivity depicted here complements previous reductive olefin coupling methods reported by Molander and Hoberg<sup>24</sup> and Baran and colleagues,<sup>25–27</sup> which proceed through organolanthanide and radical intermediates, respectively. Our mechanistic studies reveal that the unique two-electron mechanism and the radical nature of the Ni(I) catalyst are responsible for the high reductive chemoselectivity and *trans* diastereoselectivity.

## RESULTS

### Catalyst Development

Our catalyst optimization focused on dimethyl malonate-derived 1,6-heptadiene **1** as the substrate (Figure 1). The combination of Fe(acac)<sub>3</sub> and PhSiH<sub>3</sub> has been reported to reductively couple activated olefins.<sup>25</sup> This condition led to reductive cyclization of **1** to form a mixture of *cis* and *trans* diastereoisomers, with the *cis* isomer as the major product (entry 1). Conditions based on a Co catalyst developed by Crossley et al.<sup>14</sup> were ineffective for the cyclization of **1** (entry 2). ( $\alpha$ -Diimine)Ni complexes have been developed for olefin polymerization and oligomerization.<sup>28</sup> We anticipated that catalysts of this class could effect intramolecular coupling of alkenes. In the presence of Et<sub>2</sub>SiH<sub>2</sub>, ( $\text{Ar}^{\alpha}$ -diimine)NiBr<sub>2</sub> **3** (Ar = 2,6-diisopropylphenyl) catalyzed reductive cyclization of **1** in hexafluoroisopropanol (HFIP) to generate *trans*-3,4-dimethylcyclopentane **2** in 50% yield (entry 3). The reaction did not produce the *cis* diastereomer as a by-product. This exquisite selectivity for the *trans* diastereomer prompted us to investigate different catalyst precursors in order to improve the yield. ( $\alpha$ -Diimine)NiMe<sub>2</sub> **4** failed to activate and resulted in no product formation (entry 4). The extensive participation of Ni(I) and Ni(III) intermediates in

<sup>1</sup>Department of Chemistry, New York University, 100 Washington Square East, New York, NY 10003, USA

<sup>2</sup>Department of Physics and Astronomy, Hunter College, 695 Park Avenue, New York, NY 10065, USA

<sup>3</sup>Lead Contact

\*Correspondence: diao@nyu.edu

<http://dx.doi.org/10.1016/j.chempr.2017.07.010>

| Entry | Catalyst   | mol% | Silane<br>(2 equiv)                               | Yield of <b>2</b><br>(%) <sup>a</sup> |
|-------|--|------|---|---------------------------------------|
| 1     | Fe(acac) <sub>3</sub> /EtOH  | 100  | PhSiH <sub>3</sub><br>( <i>cis:trans</i> = 5.3:1) | 8                                     |
| 2     | Co(sal <sup>t</sup> Bu, <sup>t</sup> Bu)Cl   | 10   | PhSiH <sub>3</sub>                                | 0                                     |
| 3     | ( <sup>Ar</sup> $\alpha$ -diimine)Ni <sup>II</sup> Br <sub>2</sub> ( <b>3</b> )            | 5    | Et <sub>2</sub> SiH <sub>2</sub>                  | 50                                    |
| 4     | ( <sup>Ar</sup> $\alpha$ -diimine)Ni <sup>II</sup> Me <sub>2</sub> ( <b>4</b> )            | 5    | Et <sub>2</sub> SiH <sub>2</sub>                  | 0                                     |
| 5     | [( <sup>Ar</sup> $\alpha$ -diimine)Ni <sup>I</sup> ( $\mu$ -Br)] <sub>2</sub> ( <b>5</b> ) | 2.5  | Et <sub>2</sub> SiH <sub>2</sub>                  | 79                                    |
| 6     | [( <sup>Ar</sup> $\alpha$ -diimine)Ni <sup>I</sup> ( $\mu$ -H)] <sub>2</sub> ( <b>6</b> )  | 2.5  | Et <sub>2</sub> SiH <sub>2</sub>                  | 41                                    |
| 7     | [( <sup>Bn</sup> $\alpha$ -diimine)Ni <sup>II</sup> Br <sub>2</sub> ( <b>7</b> )           | 10   | Et <sub>2</sub> SiH <sub>2</sub>                  | 76                                    |
| 8     | [dtbpe]Ni <sup>I</sup> ( $\mu$ -Br)] <sub>2</sub> ( <b>8</b> )                             | 2.5  | Et <sub>2</sub> SiH <sub>2</sub>                  | 19                                    |
| 9     | [( <sup>Ar</sup> $\alpha$ -diimine)Ni <sup>I</sup> ( $\mu$ -Br)] <sub>2</sub> ( <b>5</b> ) | 2.5  | Et <sub>3</sub> SiH                               | 0                                     |
| 10    | [( <sup>Ar</sup> $\alpha$ -diimine)Ni <sup>I</sup> ( $\mu$ -Br)] <sub>2</sub> ( <b>5</b> ) | 2.5  | PhSiH <sub>3</sub>                                | 14                                    |
| 11    | [( <sup>Ar</sup> $\alpha$ -diimine)Ni <sup>I</sup> ( $\mu$ -Br)] <sub>2</sub> ( <b>5</b> ) | 2.5  | H <sub>2</sub>                                    | 0                                     |

Conditions: [1] = 0.1 M (21 mg, 0.1 mmol), hexafluoroisopropanol (HFIP) (1 mL), N<sub>2</sub>, 12 h.

<sup>a</sup> Determined by GC, internal standard = mesitylene.

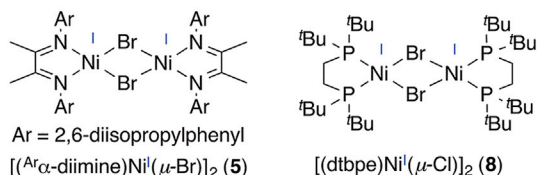


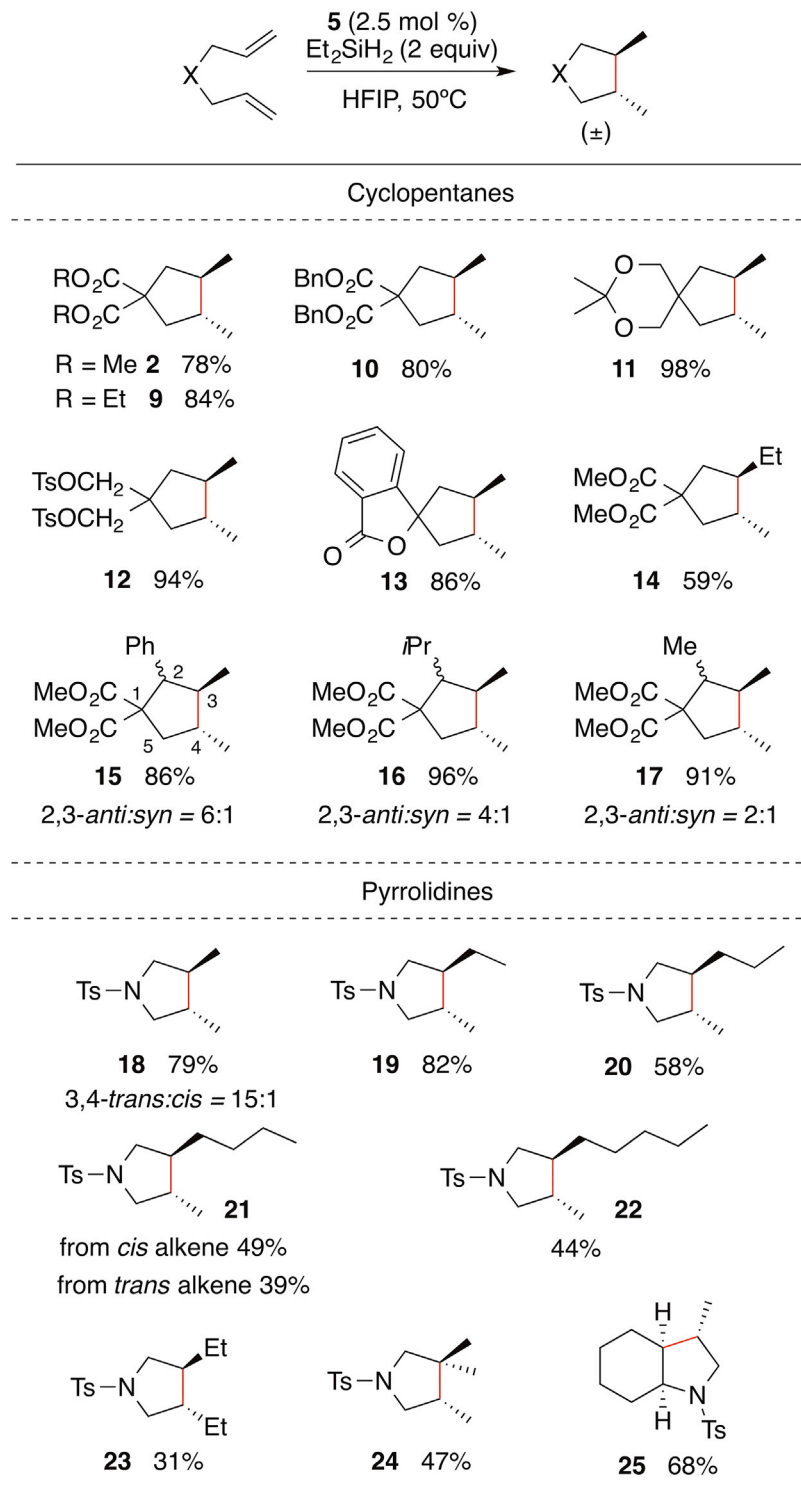
**Figure 1. Catalyst Development for Reductive Cyclization of 1,6-Diene, 1**

catalysis<sup>4</sup> led us to evaluate Ni(I) precursors. Indeed, [( $\alpha$ -diimine)Ni( $\mu$ -Br)]<sub>2</sub> **5** exhibited the highest reactivity (Figures S7 and S8),<sup>29</sup> giving rise to **2** in 79% yield (entry 5). A similar Ni(I) precursor, [( $\alpha$ -diimine)Ni( $\mu$ -H)]<sub>2</sub> **6**,<sup>30</sup> afforded **2** in a slightly lower yield (entry 6).

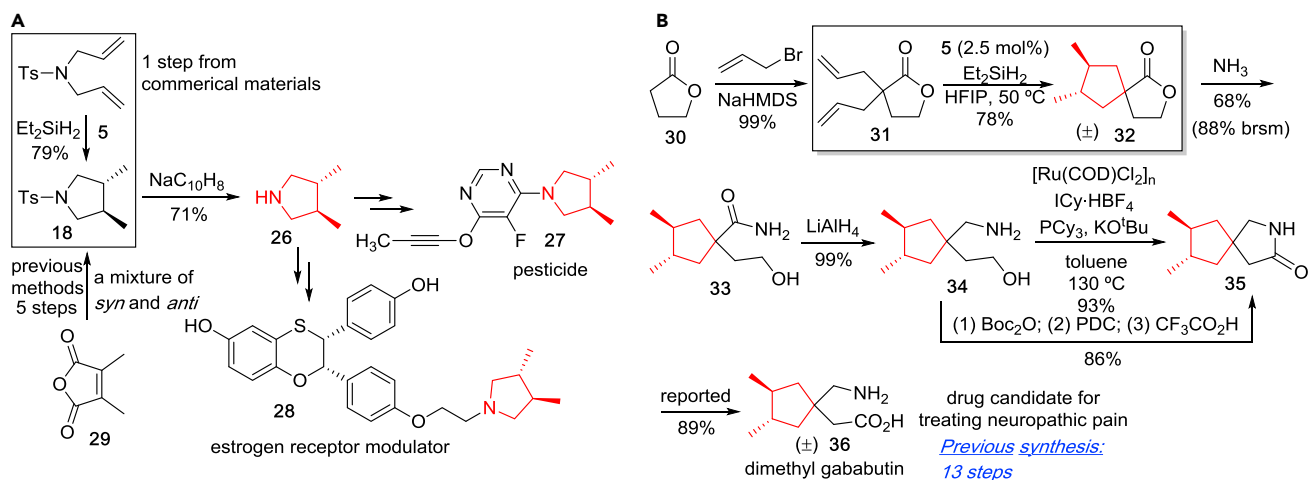
To probe the effect of ligands on this reaction, we prepared less hindered (<sup>Bn</sup> $\alpha$ -diimine)NiBr<sub>2</sub> **7**, in which the 2,6-diisopropylphenyl substituents of **5** were replaced by benzyl groups. With an increased catalyst loading of 10 mol %, we achieved a good yield of **2** with catalyst **7** (entry 7). Notably, catalyst **7** is synthetically more accessible than **5** because it requires no glovebox manipulations. [dtbpe]Ni( $\mu$ -Br)]<sub>2</sub> **8**<sup>31</sup> exhibited substantially lower reactivity than ( $\alpha$ -diimine)Ni complexes (entry 8). Evaluation of other reductants revealed that tertiary silanes (entry 9) and hydrogen were inactive (entry 11), whereas primary silanes afforded some **2** accompanied by saturated molecules resulting from the reduction of the substrate (entry 10).

## Scope

With the reaction conditions optimized, we investigated the scope of the reductive cyclization. A number of electronically unbiased 1,6-dienes (Figures S7–S20) underwent cyclization in good yields (Figure 2; see also Figures S21–S65). In all cases,

**Figure 2. Substrate Scope**

Isolated yields: unless specified, only 3,4-trans-product was observed. Solvent for 11, 18–21, and 23–25: acetone/iPrOH (5/1). Catalyst loading for 10, 20, 22, and 25 = 5 mol %. Catalyst loading for 21 = 10 mol %. NMR yield for 11 and 14: side products from the reduction and decomposition of the substrates were not separated from the cyclized product. 25: after reduction with H<sub>2</sub> in the presence of Pd/C.



**Scheme 2. Synthetic Applications of *trans*-Selective Reductive Cyclization**

(A) Derivation of *trans*-dimethyl-pyrrolidine 18 to pesticide 27 and selective estrogen receptor modulator 28.  
(B) Synthesis of dimethyl gababutin derivative 36 via Ni-catalyzed reductive cyclization.

only *trans*-3,4-disubstituted products were observed. The substrate scope generally resembles that of classic cycloisomerization reactions.<sup>10,11</sup> The Thorpe-Ingold effect is crucial to assist in the formation of cyclopentane derivatives.<sup>32</sup> The conditions tolerate a number of functional groups, including esters, acetals, and amines. When a crotyl-substituted malonate was used, the cyclization proceeded with slightly reduced reactivity to afford 14 in 59% yield. Substituents at the allylic position could give rise to 2,3-diastereoisomers on the basis of the relative positions of the substituent and the methyl groups formed. This diastereoselectivity was dependent on the size of the substituent, favoring 2,3-*anti*-diastereomers (15–17).

Cyclization of diallylamines was best performed in a mixture of acetone and iPrOH as the solvent, giving rise to a variety of pyrrolidine derivatives (18–25). 3,4-Dimethylpyrrolidine 18 formed in 15:1 diastereoselectivity, favoring the *trans* product. Substitution on the olefin exhibited a modest inhibitory effect. Cyclization of a crotyl substrate afforded pyrrolidine 19 in high yield, whereas bulkier substituents led to reduced yields (20–22). In the preparation of pyrrolidine 21, both *cis*- and *trans*-alkenes gave the desired product, but the *cis*-alkene exhibited higher reactivity. Cyclization of a dicrotyl substrate generated *trans*-diethyl pyrrolidine 23 in 31% yield, suggesting more difficult cyclization with two internal olefins. Cyclization of a geminal-disubstituted olefin proceeded to afford trisubstituted pyrrolidine 24 with a quaternary carbon in 47% yield. When a cyclohexene derivative was used as the substrate, the standard conditions gave a mixture of reductive and redox-neutral cyclization products in a 1:1 ratio, which was then converted to the single diastereomer 25 upon hydrogenation.

### Applications

The current reductive coupling reaction found appealing applications in preparing bioactive molecules. *trans*-Dimethyl-pyrrolidine product 18 can be readily deprotected to generate *trans*-3,4-dimethylpyrrolidine 26, which serves as the precursor to pesticide 27<sup>33</sup> and selective estrogen receptor modulator 28 (Scheme 2A).<sup>19</sup> Previous methods to prepare 18 require multiple steps from the commercially available dimethylmaleic anhydride 29, and give a mixture of *cis* and *trans* diastereomers.<sup>34</sup> In contrast, our cyclization reaction provides exclusive access to the *trans* diastereomer. The volatile nature of 26 prompted us to treat it with acid after deprotection

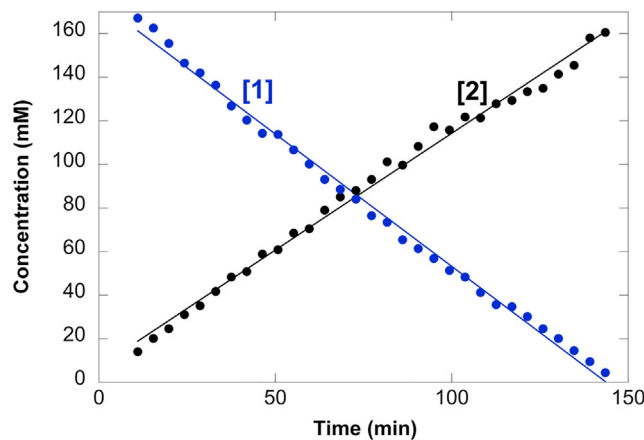


**Figure 3. Kinetic Profile of the Cyclization of 1 to Form 2**

Data were collected with  $^1\text{H}$  NMR spectroscopy. Conditions:  $[1]_0 = 167 \text{ mM}$ ,  $[\text{Et}_2\text{SiH}_2]_0 = 333 \text{ mM}$ ,  $[\text{5}] = 8.3 \text{ mM}$  (5 mol %), solvent = acetone- $d_6$  (0.5 mL) +  $i\text{PrOH-}d_6$  (0.1 mL), temperature =  $50^\circ\text{C}$ , internal standard = mesitylene.

and purify it via recrystallization (Figures S66 and S67). Resolution methods are readily available to separate the two enantiomers of 26.<sup>34</sup>

The (*R,R*) enantiomer of gababutin derivative 36 exhibits superior efficacy toward relieving neuropathic pain and anxiety in *in vivo* models (Scheme 2B).<sup>18</sup> The previous synthesis required 13 steps with less than 14% overall yield. The chiral centers were established in the first step with (–)-menthol as a chiral auxiliary.<sup>18</sup> Our reductive cyclization enables the construction of the 3,4-dimethyl cyclopentane structure 32 from the easily accessible  $\alpha,\alpha$ -dialyl-butrolactone 31 in 78% yield. Ring opening of the lactone 32 with ammonia gives amide 33 in 68% yield (88% yield on the basis of the recovered starting material). The 1,3-amino alcohol 34 undergoes dehydrogenative amide formation in the presence of a 10% Ru catalyst<sup>35</sup> to form pyrrolidone 35 in 93% yield. Alternatively, straightforward protection of the amine by  $\text{Boc}_2\text{O}$ , followed by oxidation of the alcohol by pyridinium dichromate (PDC) and deprotection of the amine, gives 35 in 86% yield over three steps (Figures S68–S79). The ring opening of 35 by acid to form 36 has been established in the previous synthetic work.<sup>18</sup> We anticipate that racemic 36 could be readily resolved to provide both enantiomers, which are both valuable for drug discovery.<sup>36</sup>

### Mechanistic Studies

Catalyst 5 displays a high chemoselectivity for reductive cyclization, as opposed to redox-neutral cycloisomerization. In addition, the reaction exhibits high diastereoselectivity favoring formation of the *trans*-disubstituted products. We conducted studies in order to elucidate the mechanistic reasons for this observed selectivity. Monitoring the conversion of 1 to 2 by *in situ*  $^1\text{H}$  nuclear magnetic resonance (NMR) spectroscopy resulted in a linear time course (Figure 3), revealing that the reaction rate was independent of  $[1]$  and  $[\text{Et}_2\text{SiH}_2]$ . We attempted to determine the kinetic isotope effect with  $\text{Et}_2\text{SiD}_2$ , but the measurements were complicated by H/D scrambling of the silane reagent with the protic solvent and the isopropyl groups of the ligand via cyclometallation, resulting in partial deuterium incorporation to the methyl groups of 2 (Figures S2 and S3). Such cyclometallation is commonplace in transition-metal-catalyzed hydrogenation and hydrosilylation reactions.<sup>37</sup>

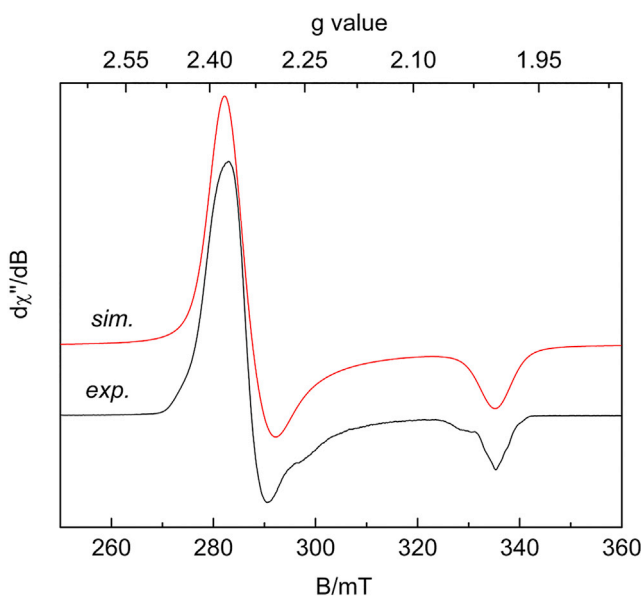


**Figure 4. X-Band EPR Spectrum of the Reaction Mixture of 1 Catalyzed by 5**

Temperature = 10 K, solvent = acetone/iPrOH (5/1). Spectroscopic parameters:  $g_x = 2.38$ ,  $g_y = 2.34$ ,  $g_z = 2.00$ ,  $A_{xx} = 5$  MHz,  $A_{yy} = 93$  MHz,  $A_{zz} = 11$  MHz. Microwave frequency = 9.380 GHz, power = 0.25 mW, modulation amplitude = 1 mT/100 kHz.

During the course of the reaction, we observed broad  $^1\text{H}$  resonances corresponding to the catalyst resting state. When the catalytic reaction was frozen, the electron paramagnetic resonance (EPR) spectrum showed a Ni-centered radical (Figure 4). The reaction catalyzed by  $(^{Bn}\alpha\text{-diimine})\text{Ni}^{\text{II}}\text{Br}_2$  7 (Figure 3, entry 7) also displayed a Ni radical signal upon freezing (Figure S1). Analyzing the crude reaction mixture revealed that  $\text{Et}_2\text{SiH(OCH(CF}_3)_2$  and  $\text{Et}_2\text{SiH(OiPr)}$  were the resulting silane products when reactions were conducted in HFIP and an acetone/iPrOH mixture, respectively.

The presence of  $S = 1/2$  Ni species, as characterized by EPR spectroscopy, prompted us to isolate possible paramagnetic Ni intermediates. We reasoned that a Ni(I)-alkyl complex could be present. We prepared  $(\alpha\text{-diimine})\text{Ni}(\text{I})\text{Bn}$  37 by taking advantage of stabilization by a cyclohexyl backbone.<sup>38</sup> Addition of  $\text{Et}_2\text{SiH}_2$  to complex 37 resulted in an immediate formation of toluene (Figure 5A). When  $\text{Et}_2\text{SiD}_2$  was used, the reaction resulted in mono-deuterated toluene. An alternative pathway for product formation involves the protonation of Ni(I)-alkyl species by protic solvents to form toluene and a Ni-alkoxyl complex. To verify this pathway, we dissolved complex 37 in a mixture of acetone- $d_6$  and iPrOH- $d_7$  in a 5/1 ratio. At 50°C, no toluene was formed in 30 min (Figure 5A).

Single-crystal X-ray diffraction established that complex 37 was stabilized by the  $\eta^3$ -coordination of the benzyl ligand (Figure 5B). Density functional theory (DFT) calculations on the electronic structure of 37 with the use of the ORCA package<sup>39</sup> suggest that the majority of the spin density is delocalized on the  $\alpha$ -diimine ligand (Figure 5C). This assignment is corroborated by its EPR spectrum, which exhibits an isotropic signal at 22°C with a  $g_{\text{iso}}$  value of 2.00 (Figure 5D). The superhyperfine splitting patterns are due to the coupling of the radical with the N ( $I = 1$ ) and  $\alpha\text{-H}$  ( $I = 1/2$ ) atoms of the ligand. Thus, the electronic structure of 37 is best described by its valence tautomer 38, featuring a Ni(II) center with a radical delocalized on the redox-active  $\alpha$ -diimine ligand (Figures 5A).<sup>40,41</sup>

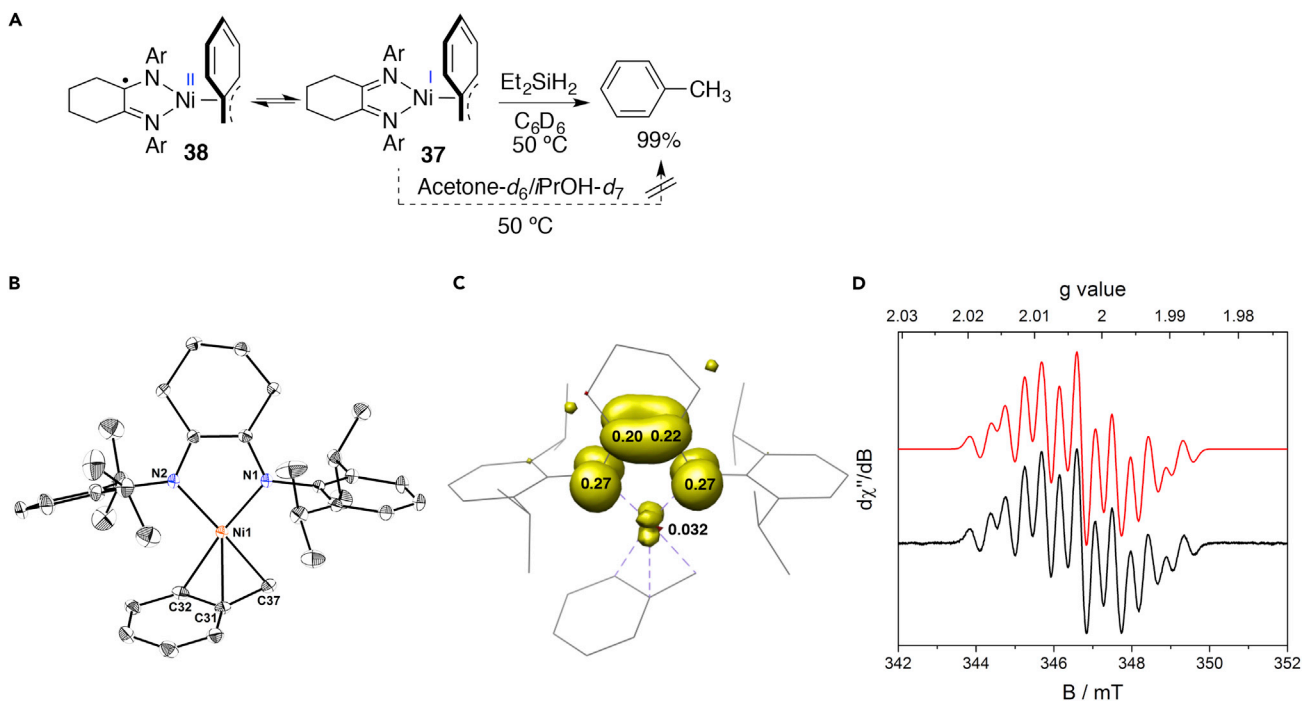


**Figure 5. Isolation and Characterization of Possible Ni(I) Intermediate 37**

- (A) Reactivity of 37 toward Et<sub>2</sub>SiH<sub>2</sub>.
- (B) Single-crystal X-ray structure of 37. Atom thermal ellipsoids were shown at the 50% probability level. Hydrogen atoms are omitted for clarity.
- (C) Mulliken spin-density plot of 37 according to DFT calculations.
- (D) X-band EPR spectrum of 37 at 22 °C. Spectroscopic parameters:  $g_{\text{iso}} = 2.003$ ,  $A(\text{N}) = 14.5$  MHz,  $A(\text{H}) = 23.5$  MHz. Microwave frequency = 9.720 GHz, power = 0.63 mW, modulation amplitude = 1 mT/100 kHz.

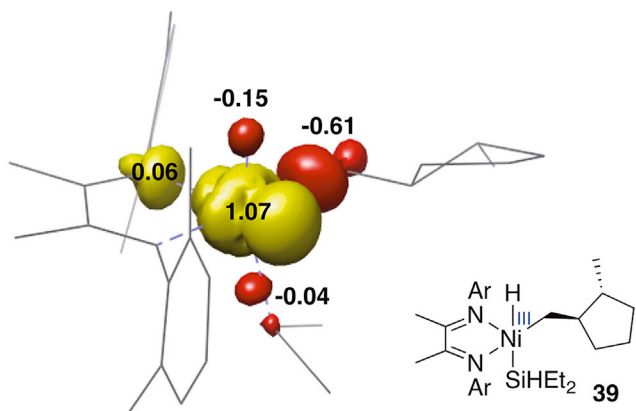
Gaussian DFT calculations on possible Ni(III) intermediates converged to square pyramidal complex 39 (Figure 6), in which the hydride and silyl groups are *trans* to each other. The spin-density plot calculated with the ORCA package<sup>39</sup> clearly shows a Ni-centered radical. Calculation of the EPR spectrum of complex 39 resulted in *g* tensors of  $g_x = 2.29$ ,  $g_y = 2.24$ , and  $g_z = 2.03$  and an  $A_{\text{iso}}$  value of 32.2 MHz.

In order to distinguish two-electron pathways from an HAT mechanism, we prepared radical clock 40 (Figures S80–S87).<sup>42</sup> Reductive cyclization of 40 generated the cyclized product 41 in 30% isolated yield, accompanied by reduced products 42 and 43 (Figure 7A; see also Figures S4, S5, and S88–S93). We attribute this side reaction to the steric hindrance created by the cyclopropyl substituent that inhibited cyclization. Importantly, the cyclopropyl group underwent no ring opening, even when the adjacent C=C double bond was reduced in 43. It is also possible that the reductive coupling proceeds via a classic cycloisomerization, followed by reduction of the unsaturated intermediate. We prepared the correspondingly exo-methylene product 45 and subjected it to our standard conditions (Figure 7B). In HFIP, internal cyclopentene was formed as the major product via migration of the C=C double bond, and cyclopentanes formed in a 2:1 *cis/trans* mixture as minor products via reduction (Figure S6). In a mixture of acetone and iPrOH, no reaction was observed.

## DISCUSSION

### Origin of *trans* Diastereoselectivity

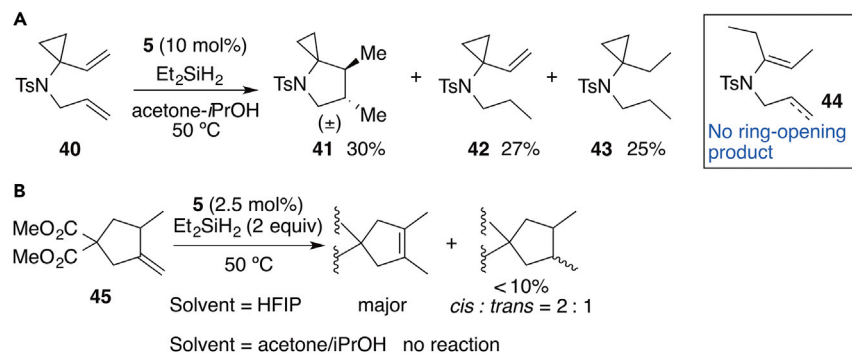
Several reasonable pathways can be proposed for the reductive cyclization of dienes (Scheme 3). Tandem cycloisomerization and reduction is expected to generate the



**Figure 6. Geometry Optimization and Spin-Density Plot of Possible Ni(III) Intermediate 39 According to DFT Calculations**

*cis* product (Scheme 3A). A control experiment in which the cycloisomerization product **45** was subjected to the reductive conditions led to olefin migration as the major product (Figure 7B) and ruled out this pathway. Cycloaddition of the diene with Ni forms a metallocycle, followed by reduction with Et<sub>2</sub>SiH<sub>2</sub> to afford the reductive cyclization product (Scheme 3B). This cycloaddition mechanism, however, would give rise to the *cis* diastereomer, as determined previously with Ni<sup>43</sup> and other metals.<sup>8</sup>

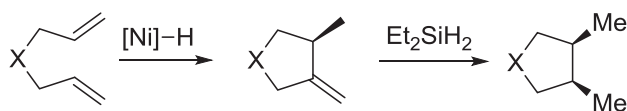
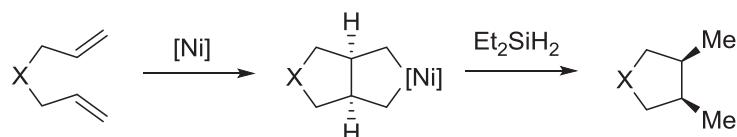
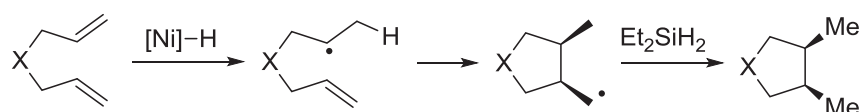
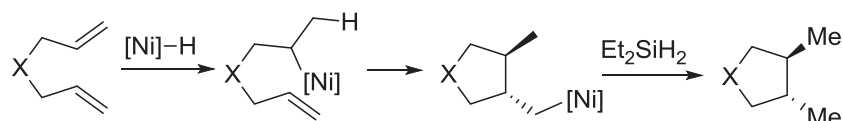
HAT pathways via organic radical intermediates have been invoked in recent olein coupling reactions.<sup>14,25,44</sup> Cyclization of diene **1** with Fe led to a mixture of *cis* and *trans* diastereomers, with a preference for the *cis* isomer (Figure 1, entry 1). The formation of the *cis* product with Fe corroborates previous studies of radical cyclization<sup>14,45</sup> and provides circumstantial evidence to exclude a radical cyclization pathway for this Ni system (Scheme 3C). In addition, results from radical clock **40** confirmed the absence of an organic radical intermediate (Figure 7A). Formation of the reduced products **42** and **43** suggests that hydride transfer occurs prior to cyclization, as opposed to formation of a radical intermediate. The observed *trans* diastereoselectivity is consistent with a classic, organometallic pathway proceeding via hydride insertion,<sup>46</sup> followed by reinsertion to the second olefin and reductive cleavage of the Ni–C bond by Et<sub>2</sub>SiH<sub>2</sub> (Scheme 3D). Previous studies in the context of cycloisomerization reveal that the hydride insertion pathway favors formation of *trans* products.<sup>47,48</sup>



**Figure 7. Mechanistic Study of Ni-Catalyzed Reductive Cyclization**

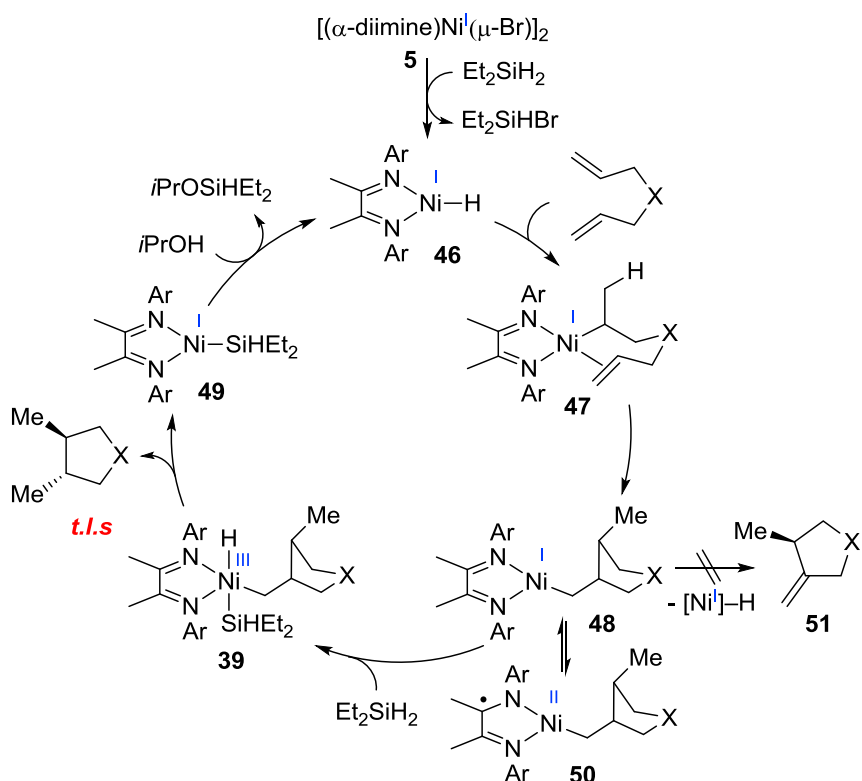
(A) Reaction of radical clock **40** under standard conditions.

(B) Control experiment of cycloisomerization product **45** under reductive cyclization conditions.

**A Cycloisomerization-Reduction****B Cycloaddition Pathway****c H-Atom Transfer Pathway****D Hydride Insertion Pathway****Scheme 3. Mechanistic Pathways for Ni-Mediated Reductive Cyclization of 1,6-Diene****Proposed Catalytic Cycle**

The *trans* diastereoselectivity and the radical clock experiment described above provide support for a classic, organometallic mechanism. Our experimental data are consistent with the catalytic cycle shown in Scheme 4, in which formal oxidation states of the Ni intermediates are shown for clarity. Activation of the dimeric catalyst 5 by  $\text{Et}_2\text{SiH}_2$  gives rise to Ni-H 46, which inserts into the diene substrate, followed by reinsertion to form Ni(I)-alkyl intermediate 48. Oxidative addition of  $\text{Et}_2\text{SiH}_2$  generates a Ni(III) intermediate 39, which undergoes reductive elimination to form the 3,4-disubstituted cyclic product and Ni-silyl 49. Ni(I)-H 46 is regenerated by the reaction of Ni-silyl intermediate 49 with the protic solvent, HFIP or *i*PrOH. The formation of the silyl ether by-product is evident after the reaction by NMR spectroscopy.

Analysis of the electronic structure of Ni(I) complex 37 suggests that the  $\alpha$ -diimine ligand is redox active, giving a Ni(II) center with an organic radical delocalized to the  $\alpha$ -diimine ligand. This assignment is consistent with the EPR spectrum of 37, showing an organic radical at 22°C (Figure 5C). In contrast, the frozen catalytic reaction displays an  $S = 1/2$  Ni species as a rhombic signal at 10 K (Figure 4). The features of the EPR spectrum resemble that of the Ni(III) complexes reported previously<sup>49–53</sup> and are consistent with the calculated EPR spectrum of Ni(III) intermediate 39 (Figure 6). Comparing the EPR spectrum of the catalyst resting state with those of known compounds suggests that the catalyst resting state is a Ni(III) species. This assignment is corroborated by the zero-order kinetic dependence on [diene] and [ $\text{Et}_2\text{SiH}_2$ ]. Thus, the turnover-limiting step is the reductive elimination of Ni(III) 39 that occurs after the insertion of the diene and addition of  $\text{Et}_2\text{SiH}_2$ . When ( $^{\text{Bn}}$  $\alpha$ -diimine)NiBr<sub>2</sub> 7 was used, the frozen reaction mixture exhibits a Ni radical (Figure S1), suggesting



**Scheme 4.** Proposed Catalytic Cycle of Ni(I)-Catalyzed Reductive Cyclization of 1,6-Dienes

that the Ni(II) precursors can be activated to access Ni(I) intermediates during the reaction. Such a catalyst activation process has been observed recently in the context of hydrosilylation.<sup>54</sup>

#### Origin of Chemoselectivity for Reductive Cyclization

The chemoselectivity of reductive cyclization in relation to cycloisomerization arises from the Ni(I)/Ni(III) catalytic cycle. The electron-rich, formal Ni(I) intermediate 48 undergoes rapid oxidative addition with Et<sub>2</sub>SiH<sub>2</sub>, which outcompetes β-H elimination to form the unsaturated cycloisomerization product 51 (Scheme 4). This chemoselectivity sharply distinguishes the Ni(I) catalyst from previous Ni(II) catalysts,<sup>10,11</sup> which favor β-H elimination rather than reaction with silanes. In addition, the lack of β-H elimination prevents possible olefin isomerization, which could lead to scrambling of the stereocenters.<sup>10,11</sup> Characterization of the electronic structure of 37 reveals that the redox-active α-diimine ligand plays an important role in stabilizing Ni(I) intermediates, such as 48, by forming its valence tautomer 50. The dtbpe ligand lacks conjugated π\* orbitals to delocalize the radical on Ni and therefore exhibits lower reactivity than α-diimine ligands (Figure 1, entry 8).

#### Conclusion

We developed a Ni-catalyzed reductive cyclization reaction of 1,6-dienes and diallyl-amines to form *trans*-3,4-disubstituted cyclopentane and pyrrolidine derivatives with high diastereoselectivity. This cyclization reaction has found applications in the preparation of biologically active molecules. The *trans* diastereoselectivity arises from a classic organometallic catalytic cycle mediated by Ni(I) and Ni(III) intermediates. The *trans* diastereoselectivity distinguishes this reaction from HAT and cyclo-addition pathways, which favor *cis* products. The electron-rich Ni(I) intermediate is

stabilized by the redox-active  $\alpha$ -diimine ligand, and is responsible for the chemoselectivity toward reductive cyclization, as opposed to redox-neutral cycloisomerization observed with previous Ni(II) catalysts. The distinct reactivity of ( $\alpha$ -diimine) Ni(I) highlights the power of ligand control in achieving unprecedented selectivity in organic transformations.

## EXPERIMENTAL PROCEDURES

Detailed experimental procedures are provided in the [Supplemental Information](#).

## ACCESSION NUMBERS

## SUPPLEMENTAL INFORMATION

补充信息包括补充实验程序、93幅图和2个数据文件，可以在<http://dx.doi.org/10.1016/j.chempr.2017.07.010>找到。

## AUTHOR CONTRIBUTIONS

Y.K., D.A., and F.M. performed the experiments. J.K. conducted the DFT calculations of intermediate 39. S.H. performed the EPR characterization of compound 32. T.D. supervised the project and wrote the manuscript.

## ACKNOWLEDGMENTS

我们感谢Nadia Leonard (Chirik实验室, Princeton University) 和 Prof. Steven Greenbaum (Hunter College) 在协助录制EPR光谱方面提供的帮助; Dr. Chunhua Hu 在解决化合物 5 和 37 的晶体结构方面提供了帮助; Prof. Carsten Milsmann (University of West Virginia) 在讨论中提供了有益的帮助。该研究得到了美国化学会石油基金(56568-DNI3)和纽约大学的资助。

收到: 2017年5月17日

修订: 2017年6月24日

接受: 2017年7月20日

发表: 2017年8月10日

## REFERENCES

- Tasker, S.Z., Standley, E.A., and Jamison, T.F. (2014). Recent advances in homogeneous nickel catalysis. *Nature* 509, 299–309.
- Choi, J., and Fu, G.C. (2017). Transition metal-catalyzed alkyl-alkyl bond formation: another dimension in cross-coupling chemistry. *Science* 356, <http://dx.doi.org/10.1126/science.aaf7230>.
- For a review of the mechanism of Ni-catalyzed reactions, see: Hu, X. (2011). Nickel-catalyzed cross coupling of non-activated alkyl halides: a mechanistic perspective. *Chem. Sci.* 2, 1867–1886.
- Yan, M., Lo, J.C., Edwards, J.T., and Baran, P.S. (2016). Radicals: reactive intermediates with translational potential. *J. Am. Chem. Soc.* 138, 12692–12714.
- Jackson, E.P., Malik, H.A., Sormunen, G.J., Baxter, R.D., Liu, P., Wang, H., Shareef, A.-R., and Montgomery, J. (2015). Mechanistic basis for regioselection and regiodivergence in nickel-catalyzed reductive couplings. *Acc. Chem. Res.* 48, 1736–1745.
- Fu, G.C., Nguyen, S.T., and Grubbs, R.H. (1993). Catalytic ring-closing metathesis of functionalized dienes by a ruthenium carbene complex. *J. Am. Chem. Soc.* 115, 9856–9857.
- Alexander, J.B., La, D.S., Cefalo, D.R., Hoveyda, A.H., and Schrock, R.R. (1998). Catalytic enantioselective ring-closing metathesis by a chiral biphen-mo complex. *J. Am. Chem. Soc.* 120, 4041–4042.
- Bouwkamp, M.W., Bowman, A.C., Lobkovsky, E., and Chirik, P.J. (2006). Iron-catalyzed  $[2\pi + 2\pi]$  cycloaddition of  $\alpha,\omega$ -dienes: the importance of redox-active supporting ligands. *J. Am. Chem. Soc.* 128, 13340–13341.
- Xia, Q., and Ganem, B. (2001). Asymmetric total synthesis of (-)- $\alpha$ -kainic acid using an enantioselective, metal-promoted ene cyclization. *Org. Lett.* 3, 485–487.
- Widenhoefer, R.A. (2002). Synthetic and mechanistic studies of the cycloisomerization and cyclization/hydrosilylation of functionalized dienes catalyzed by cationic palladium(II) complexes. *Acc. Chem. Res.* 35, 905–913.
- Yamamoto, Y. (2012). Transition-metal-catalyzed cycloisomerizations of  $\alpha,\omega$ -dienes. *Chem. Rev.* 112, 4736–4769.
- Widenhoefer, R.A., and DeCarli, M.A. (1998). Tandem cyclization/hydrosilylation of functionalized 1,6-dienes catalyzed by a cationic palladium complex. *J. Am. Chem. Soc.* 120, 3805–3806.

13. Perch, N.S., Pei, T., and Widenhoefer, R.A. (2000). Enantioselective diene cyclization/hydrosilylation catalyzed by optically active palladium bisoxazoline and pyridine–oxazoline complexes. *J. Org. Chem.* 65, 3836–3845.
14. Crossley, S.W.M., Barabé, F., and Shenvi, R.A. (2014). Simple, chemoselective, catalytic olefin isomerization. *J. Am. Chem. Soc.* 136, 16788–16791.
15. Nguyen, K.D., Park, B.Y., Luong, T., Sato, H., Garza, V.J., and Krische, M.J. (2016). Metal-catalyzed reductive coupling of olefin-derived nucleophiles: reinventing carbonyl addition. *Science* 354, <http://dx.doi.org/10.1126/science.aah5133>.
16. Chen, M., Weng, Y., Guo, M., Zhang, H., and Lei, A. (2008). Nickel-catalyzed reductive cyclization of unactivated 1,6-enynes in the presence of organozinc reagents. *Angew. Chem. Int. Ed.* 47, 2279–2282.
17. Perch, N.S., Kisanga, P., and Widenhoefer, R.A. (2000). Reductive cyclization of dimethyl diallylmalonate catalyzed by palladium–bisoxazoline complexes in the presence of silane and water. *Organometallics* 19, 2541–2545.
18. Blakemore, D.C., Bryans, J.S., Carnell, P., Field, M.J., Kinsella, N., Kinsora, J.K., Meltzer, L.T., Osborne, S.A., Thompson, L.R., and Williams, S.C. (2010). Synthesis and *in vivo* evaluation of 3,4-disubstituted gababutins. *Biorg. Med. Chem. Lett.* 20, 248–251.
19. Blizzard, T.A., DiNinno, F., Morgan Li, J.D., Chen, H.Y., Wu, J.Y., Kim, S., Chan, W., Birzin, E.T., Yang, Y.T., Pai, L.-Y., et al. (2005). Estrogen receptor ligands. Part 9: dihydrobenzoxathiin SERMs with alkyl substituted pyrrolidine side chains and linkers. *Biorg. Med. Chem. Lett.* 15, 107–113.
20. Zhuang, S., Zhang, J., Zhang, F., Zhang, Z., Wen, Y., and Liu, W. (2011). Investigation of the diastereomerism of dihydrobenzoxathiin SERMs for ER alpha by molecular modeling. *Biorg. Med. Chem. Lett.* 21, 7298–7305.
21. Curran, D.P., and Shen, W. (1993). Radical translocation reactions of vinyl radicals: substituent effects on 1,5-hydrogen-transfer reactions. *J. Am. Chem. Soc.* 115, 6051–6059.
22. Kochi, T., Hamasaki, T., Aoyama, Y., Kawasaki, J., and Kakiuchi, F. (2012). Chain-walking strategy for organic synthesis: catalytic cycloisomerization of 1,n-dienes. *J. Am. Chem. Soc.* 134, 16544–16547.
23. Knight, K.S., and Waymouth, R.M. (1991). Zirconium-catalyzed diene and alkyl-alkene coupling reactions with magnesium reagents. *J. Am. Chem. Soc.* 113, 6268–6270.
24. Molander, G.A., and Hoberg, J.O. (1992). Organoyttrium-catalyzed cyclization of substituted 1,5- and 1,6-dienes. *J. Am. Chem. Soc.* 114, 3123–3125.
25. Lo, J.C., Gui, J., Yabe, Y., Pan, C.-M., and Baran, P.S. (2014). Functionalized olefin cross-coupling to construct carbon–carbon bonds. *Nature* 516, 343–348.
26. Lo, J.C., Yabe, Y., and Baran, P.S. (2014). A practical and catalytic reductive olefin coupling. *J. Am. Chem. Soc.* 136, 1304–1307.
27. Lo, J.C., Kim, D., Pan, C.-M., Edwards, J.T., Yabe, Y., Gui, J., Qin, T., Gutiérrez, S., Giacoboni, J., Smith, M.W., et al. (2017). Fe-catalyzed C–C bond construction from olefins via radicals. *J. Am. Chem. Soc.* 139, 2484–2503.
28. Johnson, L.K., Killian, C.M., and Brookhart, M. (1995). New Pd(II)- and Ni(II)-based catalysts for polymerization of ethylene and  $\alpha$ -olefins. *J. Am. Chem. Soc.* 117, 6414–6415.
29. Meinhard, D., Reuter, P., and Rieger, B. (2007). Activation of polymerization catalysts: synthesis and characterization of novel dinuclear nickel(I) diimine complexes. *Organometallics* 26, 751–754.
30. Dong, Q., Zhao, Y., Su, Y., Su, J.-H., Wu, B., and Yang, X.-J. (2012). Synthesis and reactivity of nickel hydride complexes of an  $\alpha$ -diimine ligand. *Inorg. Chem.* 51, 13162–13170.
31. Mindiola, D.J., and Hillhouse, G.L. (2001). Terminal amido and imido complexes of three-coordinate nickel. *J. Am. Chem. Soc.* 123, 4623–4624.
32. Jung, M.E., and Piuzzi, G. (2005). gem-Disubstituent effect: theoretical basis and synthetic applications. *Chem. Rev.* 105, 1735–1766.
33. Hajime, M., and Akio, M. (2004). Pyrimidine compounds and pests controlling composition containing the same. Patent WO2004099160 A1, filed May 10, 2004, and published November 18, 2004.
34. Punniyamurthy, T., and Katsuki, T. (1999). Asymmetric desymmetrization of meso-pyrrolidine derivatives by enantiotopic selective C–H hydroxylation using (salen) manganese(III) complexes. *Tetrahedron* 55, 9439–9454.
35. Nordström, L.U., Vogt, H., and Madsen, R. (2008). Amide synthesis from alcohols and amines by the extrusion of dihydrogen. *J. Am. Chem. Soc.* 130, 17672–17673.
36. Bhushan, R., and Ali, I. (1987). Resolution of enantiomeric mixtures of phenylthiohydantoin amino acids on (+)-tartaric acid-impregnated silica gel plates. *J. Chromatogr. A* 392, 460–463.
37. Bart, S.C., Lobkovsky, E., and Chirik, P.J. (2004). Preparation and molecular and electronic structures of iron(0) dinitrogen and silane complexes and their application to catalytic hydrogenation and hydrosilation. *J. Am. Chem. Soc.* 126, 13794–13807.
38. Xu, H., White, P.B., Hu, C., and Diao, T. (2017). Structure and isotope effects of the  $\beta$ -H agostic ( $\alpha$ -diimine)nickel cation as a polymerization intermediate. *Angew. Chem. Int. Ed.* 56, 1535–1538.
39. Neese, F. (2012). The ORCA program system. *WIREs Comput. Mol. Sci.* 2, 73–78.
40. Chirik, P.J., and Wieghardt, K. (2010). Radical ligands confer nobility on base-metal catalysts. *Science* 327, 794–795.
41. Khusnutdinova, J.R., and Milstein, D. (2015). Metal-ligand cooperation. *Angew. Chem. Int. Ed.* 54, 12236–12273.
42. Griller, D., and Ingold, K.U. (1980). Free-radical clocks. *Acc. Chem. Res.* 13, 317–323.
43. Sato, Y., Saito, N., and Mori, M. (2000). A novel asymmetric cyclization of  $\omega$ -formyl-1,3-dienes catalyzed by a zerovalent nickel complex in the presence of silanes. *J. Am. Chem. Soc.* 122, 2371–2372.
44. Obradors, C., Martinez, R.M., and Shenvi, R.A. (2016). Ph(*i*-PrO)SiH<sub>2</sub>: an exceptional reductant for metal-catalyzed hydrogen atom transfers. *J. Am. Chem. Soc.* 138, 4962–4971.
45. Kuo, J.L., Hartung, J., Han, A., and Norton, J.R. (2015). Direct generation of oxygen-stabilized radicals by H• transfer from transition metal hydrides. *J. Am. Chem. Soc.* 137, 1036–1039.
46. Diccianni, J.B., Heitmann, T., and Diao, T. (2017). Nickel-catalyzed reductive cycloisomerization of enynes with CO<sub>2</sub>. *J. Org. Chem.* 82, 6895–6903.
47. Goj, L.A., and Widenhoefer, R.A. (2001). Mechanistic studies of the cycloisomerization of dimethyl diallylmalonate catalyzed by a cationic palladium phenanthroline complex. *J. Am. Chem. Soc.* 123, 11133–11147.
48. Perch, N.S., and Widenhoefer, R.A. (2004). Mechanism of palladium-catalyzed diene cyclization/hydrosilylation: direct observation of intramolecular carbometalation. *J. Am. Chem. Soc.* 126, 6332–6346.
49. Zhang, C.-P., Wang, H., Klein, A., Biewer, C., Stirnat, K., Yamaguchi, Y., Xu, L., Gomez-Benitez, V., and Vicic, D.A. (2013). A five-coordinate nickel(II) fluoroalkyl complex as a precursor to a spectroscopically detectable Ni(III) species. *J. Am. Chem. Soc.* 135, 8141–8144.
50. Zheng, B., Tang, F., Luo, J., Schultz, J.W., Rath, N.P., and Mirica, L.M. (2014). Organometallic nickel(III) complexes relevant to cross-coupling and carbon–heteroatom bond formation reactions. *J. Am. Chem. Soc.* 136, 6499–6504.
51. Xu, H., Diccianni, J.B., Katigbak, J., Hu, C., Zhang, Y., and Diao, T. (2016). Bimetallic C–C bond-forming reductive elimination from nickel. *J. Am. Chem. Soc.* 138, 4779–4786.
52. Diccianni, J.B., Hu, C., and Diao, T. (2017). Binuclear, high-valent nickel complexes: Ni–Ni bonds in aryl–halogen bond formation. *Angew. Chem. Int. Ed.* 56, 3635–3639.
53. Bour, J.R., Camasso, N.M., Meucci, E.A., Kampf, J.W., Carty, A.J., and Sanford, M.S. (2016). Carbon–carbon bond-forming reductive elimination from isolated Nickel(III) complexes. *J. Am. Chem. Soc.* 138, 16105–16111.
54. Pappas, I., Treacy, S., and Chirik, P.J. (2016). Alkene hydrosilylation using tertiary silanes with  $\alpha$ -diimine nickel catalysts. redox-active ligands promote a distinct mechanistic pathway from platinum catalysts. *ACS Catal.* 4105–4109.